THE JOURNAL OF BIOLOGICAL CHEMISTRY VOL. 287, NO. 16, pp. 12679–12690, April 13, 2012

ATP-dependent Mitochondrial Porphyrin Importer ABCB6 Protects against Phenylhydrazine Toxicity*[S]

Received for publication, December 21, 2011, and in revised form, January 30, 2012 Published, JBC Papers in Press, January 31, 2012, DOI 10.1074/jbc.M111.336180

Dagny L. Ulrich[‡], John Lynch[‡], Yao Wang[‡], Yu Fukuda[‡], Deepa Nachagari[‡], Guoqing Du[‡], Daxi Sun[‡], Yiping Fan[§], Lyudmila Tsurkan[¶], Philip M. Potter[¶], Jerold E. Rehg[‖], and John D. Schuetz[‡1]

From the Departments of [‡]Pharmaceutical Sciences, [§]Research Informatics, [¶]Chemical Biology and Therapeutics, and [‖]Pathology, St. Jude Children's Research Hospital, Memphis, Tennessee 38105

Background: The role of the mitochondrial ABC transporter, Abcb6, *in vivo* is unknown.
Results: Abcb6-null mice are incapable of ATP-dependent import of mitochondrial porphyrins. Despite compensatory changes in the porphyrin pathway, Abcb6-null mice are less viable after a porphyrin-inducing stress.
Conclusion: Abcb6 absence abolished ATP-dependent mitochondrial porphyrin uptake and deregulated porphyrin pathway genes.
Significance: Disrupted Abcb6 function may produce porphyria after certain stresses.

Abcb6 is a mammalian mitochondrial ATP-binding cassette (ABC) transporter that regulates *de novo* porphyrin synthesis. In previous studies, haploinsufficient ($Abcb6^{+/-}$) embryonic stem cells showed impaired porphyrin synthesis. Unexpectedly, $Abcb6^{-/-}$ mice derived from these stem cells appeared phenotypically normal. We hypothesized that other ATP-dependent and/or -independent mechanisms conserve porphyrins. Here, we demonstrate that $Abcb6^{-/-}$ mice lack mitochondrial ATP-driven import of coproporphyrin III. Gene expression analysis revealed that loss of Abcb6 results in up-regulation of compensatory porphyrin and iron pathways, associated with elevated protoporphyrin IX (PPIX). Phenylhydrazine-induced stress caused higher mortality in $Abcb6^{-/-}$ mice, possibly because of sustained elevation of PPIX and an inability to convert PPIX to heme despite elevated ferrochelatase levels. Therefore, Abcb6 is the sole ATP-dependent porphyrin importer, and loss of Abcb6 produces up-regulation of heme and iron pathways necessary for normal development. However, under extreme demand for porphyrins (*e.g.* phenylhydrazine stress), these adaptations appear inadequate, which suggests that under these conditions Abcb6 is important for optimal survival.

ATP-binding cassette (ABC)[2] transporters move structurally diverse compounds across membranes. We recently demonstrated that the mitochondrial ABC transporter ABCB6 activates *de novo* heme and porphyrin biosynthesis and elevates intracellular protoporphyrin IX (PPIX), whereas the loss of one *Abcb6* allele in embryonic stem (ES) cells impairs porphyrin synthesis (1). Porphyrin synthesis requires the coordination of cellular and mitochondrial processes, as the initial steps require precursors from the Krebs cycle and the terminal step requires that ferrous iron (Fe^{2+}) be delivered to the mitochondria and added via ferrochelatase (FECH) catalysis to the PPIX ring to complete heme formation. It is currently unknown whether Abcb6 is required for normal basal porphyrin synthesis or instead has a more selective role during high demand for porphyrin precursors (*e.g.* during stress erythropoiesis).

Here, we present the first evidence that Abcb6 is the only ATP-dependent mitochondrial importer of porphyrins. For example, ATP-driven import of such porphyrins such as coproporphyrin III (CP), is completely absent in the mitochondria of $Abcb6^{-/-}$ mice, whereas non-ATP-dependent mitochondrial CP uptake is identical in $Abcb6^{-/-}$ and wild-type mice. Moreover, there is no evident functional up-regulation of other potential mitochondrial porphyrin importers, such as peripheral benzodiazepine receptor (also known as TSPO), 2-oxoglutarate carrier (also known as SLC25a11), the adenine nucleotide translocator (ANT1), and voltage-dependent anion channel, in the absence of Abcb6 (2–6). In addition, constitutive absence of Abcb6 results in increased expression of genes important for porphyrin biosynthesis (*e.g.* SLC48a) (7) and iron homeostasis (*e.g.* SLC25a37) (8) in erythroid cells. During phenylhydrazine toxicity, genes important for porphyrin and iron conservation are up-regulated in wild-type mice but not in *Abcb6*-null mice. Taken together, our findings suggest that although Abcb6 is not essential for basal porphyrin synthesis, it has an important role in coordinating heme and iron homeostasis during times when high porphyrin demand occurs such as during phenylhydrazine stress.

EXPERIMENTAL PROCEDURES

Generation of ES Cells Expressing Nonfunctional Abcb6—An Abcb6-targeting vector was constructed in the pKO vector by standard molecular procedures. Briefly, the 5′ arm consisted of a 3.2-kb HindIII/XhoI fragment 5′ of *Abcb6* exon 6 ligated into the pKONTKV1901 vector (Stratagene). The 3′ arm was a

* This work was supported, in whole or in part, by National Institutes of Health Grants ES058571, P30 CA21745, and CA21865. This work was also supported by American Lebanese Syrian Associated Charities.
[S] This article contains supplemental Figs. S1–S6, Tables S1–S4, "Materials and Methods," and additional references.
[1] To whom correspondence should be addressed: Dept. of Pharmaceutical Sciences, MS 313, St. Jude Children's Research Hospital, 262 Danny Thomas Place, Memphis, TN 38105-3678. Tel.: 901-595-2174; Fax: 901-595-3125; E-mail: John.Schuetz@stjude.org.
[2] The abbreviations used are: ABC, ATP-binding cassette; FECH, ferrochelatase; HMBA, hexamethylenebisacetamide; ZnPP, zinc-protoporphyrin; Phz, phenylhydrazine; ISC, iron-sulfur cluster; AMP-PNP, adenosine 5′-(β,γ-imino)triphosphate.

5.4-kb EcoRI fragment of *Abcb6* containing exons 16–19. The fragments were verified by DNA sequence analysis. The targeting vector was linearized with NotI and electroporated into 129/SVJ-derived ES cells. Genomic DNA from 798 ES clones that survived 2 weeks of G418 selection was screened first by PCR analysis and subsequently by Southern blot analysis.

Animals—All procedures involving animals were approved by the St. Jude IAUCAC committee. All mice were born and housed in the St. Jude Children's Research Hospital animal care facility. Mice were maintained on a standard rodent diet. In these experiments, littermates were used as controls.

Coproporphyrin III Uptake Assay—Mitochondria were isolated from livers of female mice, prepared as described (9, 10), and used immediately. Mitochondria (50–100 μg) were resuspended in Tris-sucrose (TS) buffer (50 mM Tris-HCl, 250 mM sucrose, pH 7.4) (final volume, 50 μl). Equal volumes of reaction mix and control mix were freshly prepared for each assay. Reactions (in triplicate) were started by adding 50 μl of reaction or control mix to each sample and incubated the time interval indicated at 37 °C. Reactions were stopped by dilution with 1 ml of ice-cold TS buffer, and samples were stored on ice. Blanks were prepared by adding mitochondria and reaction/control mix directly to 1 ml of ice-cold TS buffer and incubating on ice. Samples were centrifuged at 16,000 $\times$ *g* in a refrigerated tabletop centrifuge for 5 min, and the pellet was washed twice with ice-cold TS buffer. Pellets were lysed by incubation for 10 min in 1% Nonidet P-40 solution with agitation, and fluorescence was measured at excitation wavelength 405 nm and emission wavelength 630 nm. Concentration of CP was determined from a standard curve of CP in 1% Nonidet P-40. The rate of active transport (pmol·min^{-1} mg^{-1}) was calculated as the difference between ATP-dependent and -independent uptake.

Determination of Kinetic Constants—K_m and V_{max} values were determined for coproporphyrin transport using a combination of two methods. First, the transport rates *versus* CP concentration graphs were transposed to generate Lineweaver-Burke graphs and values of K_m and V_{max} estimated by linear regression analysis. To confirm these estimates, nonlinear regression was conducted using GraphPad Prism version 5.00 for Windows (GraphPad Software, San Diego). The values obtained by these two methods varied by less than 10%.

Analysis of Expression Screening—Gene expression screening was based on the methods of Nilsson *et al.* (11). Freely available mammalian microarray data were used to search for genes consistently coexpressed with a query dataset. 15 GEO datasets (314 chips) were obtained from the NCBI Gene Expression Omnibus between September and December 2009. A prior p_0 value of 15% (*versus* 5% in the Nilsson method) was used to calculate the integrated *p* value, as we started from a more narrowly defined list of genes (those up-regulated in *Abcb6*$^{-/-}$ erythroblasts). We used the following eight heme biosynthetic genes as controls: *alad, alas2, cpox, fech, hmbs, ppox, urod*, and *uros*. The gene expression value in each data set was calculated by using the Affymetrix MAS5 method. We mapped Affymetrix probe sets in the Affymetrix Mouse 430_2 array to other Affymetrix array platforms, using either the best matched probe or probe ortholog files available from the Affymetrix web site. When multiple probe sets were applicable to genes, those with the maximum expression values were used. The probability of coexpression of each gene with the eight known heme genes was calculated within each dataset, and the genes were ranked in order of their likelihood of coexpression with the heme genes. The dataset weight (w_d) was defined as the mean coexpression probability across the eight heme genes.

For the heat map showing *Abcb6* expression throughout erythroid differentiation, the dataset GSE4655 (erythroid differentiation *in vitro*, *Homo sapiens*) was used. Heat maps were generated on the basis of Z-scores, calculated as $Z = (x - m)/s$, where x is the raw gene expression value to be standardized; m is the mean gene expression across all samples, and s is the corresponding standard deviation.

HPLC Measurement of PPIX, ZnPP, and Heme—Samples of peripheral blood mixed with EDTA were lysed in the HPLC mobile phase (described below) for 30 min at room temperature and then centrifuged (50,000 $\times$ *g*) for 10 min at 4 °C. Twenty microliters of supernatant was injected into the HPLC system (Beckman System Gold Programmable Solvent Module 126). ZnPP and PPIX were separated on a Hibar 125 $\times$ 4-mm LiChrospher 100 RP-18 column (5 μm; Merck) with a mobile phase containing 10% 1 M ammonium acetate buffer, pH 5.0, 30% methanol, and 60% (v/v) acetonitrile at a flow rate of 1 ml/min. ZnPP and PPIX were detected by fluorescence (ZnPP, excitation 415 nm and emission 590 nm; PPIX, excitation 405 nm and emission 630 nm). Under these conditions, ZnPP and PPIX were eluted at 2.5 and 6.1 min, respectively. Results were quantified by comparison to known quantities of external standards.

For heme and porphyrin analysis, porphyrins were extracted from whole-blood samples with acidified acetone and centrifuged at 16,000 $\times$ *g* for 10 min. Heme was separated from other porphyrins on a Shimadzu system, using a mobile phase of acetonitrile in water containing 0.05% trichloroacetic acid at 1 ml/min on a reverse-phase C18 column (MC Medical), applying a 30–66% linear gradient over 5 min followed by a 66–90% linear gradient over 20 min. Heme absorbance was read at 400 nm, whereas porphyrin fluorescence was measured at 395 nm (excitation) and 630 nm (emission). The heme/ZnPP ratio of each sample was determined by dividing the heme absorbance by the PPIX fluorescence. The heme absorbance value of each sample was normalized to the absolute reticulocyte count (as determined by both Ter119 and thiazole-orange double-positive cells).

Erythroid Krüppel-like Transcription Factor (EKLF Also Known as KLF1) Binding Site Analysis—EKLF binds specifically to the sequence CCACACCCT (12) and loosely to the sequence CCNCNCCCN (13) (core binding sequence, CACCC) (14). For each of the 71 submitted query genes, 3 kb of upstream sequence plus 5′-UTR were derived from the UCSC genome browser. Three EKLF binding patterns were mapped by using DNA pattern analysis and visualized by using Feature map in the RSA suite of tools (15).

RESULTS

Abcb6 Knock-out and Expression—*Abcb6* comprises 19 exons and is highly conserved in humans and mice (16). *Abcb6* was disrupted in embryonic stem (ES) cells by using homolo-

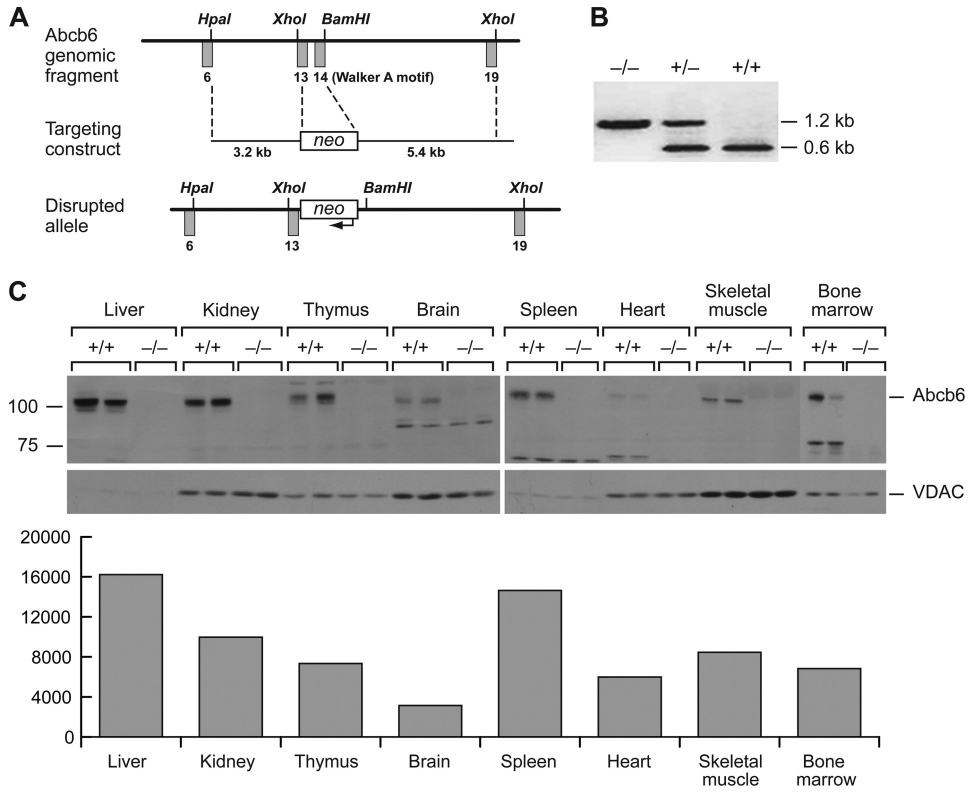

FIGURE 1. **Generation of *Abcb6*$^{-/-}$ mice.** *A*, construct used. *B*, PCR analysis of genomic DNA from wild-type, *Abcb6*$^{+/-}$, and *Abcb6*$^{-/-}$ mice. The wild-type allele amplifies a 0.6-kb fragment and the null allele a 1.2-kb fragment. *C*, Western blot (*upper panel*) and quantitative graph (*lower panel*) of Abcb6 in mitochondria isolated from various tissues of adult *Abcb6*$^{-/-}$ mice. A separate gel was used for bone marrow lysates. *VDAC*, voltage-dependent anion channel.

gous recombination to replace exons 13 and 14 (encoding the Walker A ATP-binding motif essential for ABC transporter function) (17) with the neomycin resistance cassette (Fig. 1*A*), as verified by PCR (Fig. 1*B*). Immunoblot analysis of mitochondrial lysates from various tissues revealed a gene dose effect, *i.e.* loss of one allele reduced Abcb6 protein by half (supplemental Fig. S1). After normalization with the mitochondrial protein voltage-dependent anion channel, Abcb6 was highly expressed in the mitochondria of multiple tissues, most highly in the liver and spleen (Fig. 1*C*). In several tissues (bone marrow and heart), substantial proteolytic cleavage of Abcb6 resulted in a reduced size immunoreactive band.

Abcb6$^{-/-}$ *Mice Lack ATP-driven Coproporphyrin III Mitochondrial Import*—Among the porphyrins that interact with Abcb6, CP was a prime candidate substrate because it potently disrupted the hemin-agarose interaction with Abcb6 and inhibited heme import into mitochondria (17). Although CP differs electronically from the endogenous substrate coproporphyrinogen III, the main feature distinguishing the porphyrins interacting with Abcb6 is the tetratrapyrrole structure (17). Furthermore, unlike coproporphyrinogen III, which is highly susceptibility to oxidation and not suitable for isolated mitochondrial transport assays, CP is a stable substrate that is very similar to the endogenous coproporphyrinogen III. Mitochondrial CP uptake assays have been described previously (18, 19). However, these studies did not provide unequivocal evidence for CP transport because they either did not include ATP or the concentrations were exceedingly high. To determine the kinetics of CP binding and transport, we developed a CP uptake assay using hepatic mitochondria from adult wild-type and *Abcb6*$^{-/-}$ mice. We utilized the nonhydrolyzable ATP analog AMP-PNP to distinguish between ATP-dependent (requiring ATP hydrolysis) and nondependent import (Fig. 2*A*). The wild-type and *Abcb6*$^{-/-}$ mice showed nearly identical non-ATP-dependent CP uptake (4.5 ± 0.9 and 5.4 ± 1.8 pmol/mg, respectively). In contrast, ATP-dependent transport (~4 pmol/min/mg) was measurable only in the wild-type mice. In the wild-type mice, ATP-dependent CP transport was saturable and displayed Michaelis-Menten kinetics with a V_{max} of 9.8 pmol·min^{-1} mg^{-1} and a K_m of 12.6 μM (Fig. 2*B*).

We hypothesized that Abcb6 up-regulation is required to meet the increased demand for porphyrins during erythropoiesis. We tested this hypothesis in an immortalized erythroid cell line, the murine MEL cells, which can be induced by hexamethylenebisacetamide (HMBA) to activate heme/porphyrin synthesis. MEL cells were untreated or treated with HMBA for 120 h before mitochondrial isolation. The initial rate of ATP-dependent CP transport was four times as great in HMBA-treated cells (18.24 pmol·min^{-1} mg^{-1}) as in untreated cells (4.67 pmol·min^{-1} mg^{-1}) (Fig. 2*C*, *upper panel*). In contrast, non-ATP-dependent CP uptake was almost identical in treated and untreated MEL cells (Fig. 2*C*, *lower panel*). Quantitative analysis indicated that mitochondrial expression of Abcb6 was increased by a factor of ~5 by HMBA treatment. Although the expression of peripheral benzodiazepine receptor (an energy-independent porphyrin importer) also increased in HMBA-treated MEL cells (Fig. 2*D*), it did not appear to substantially contribute to the ATP-independent import of CP, consistent

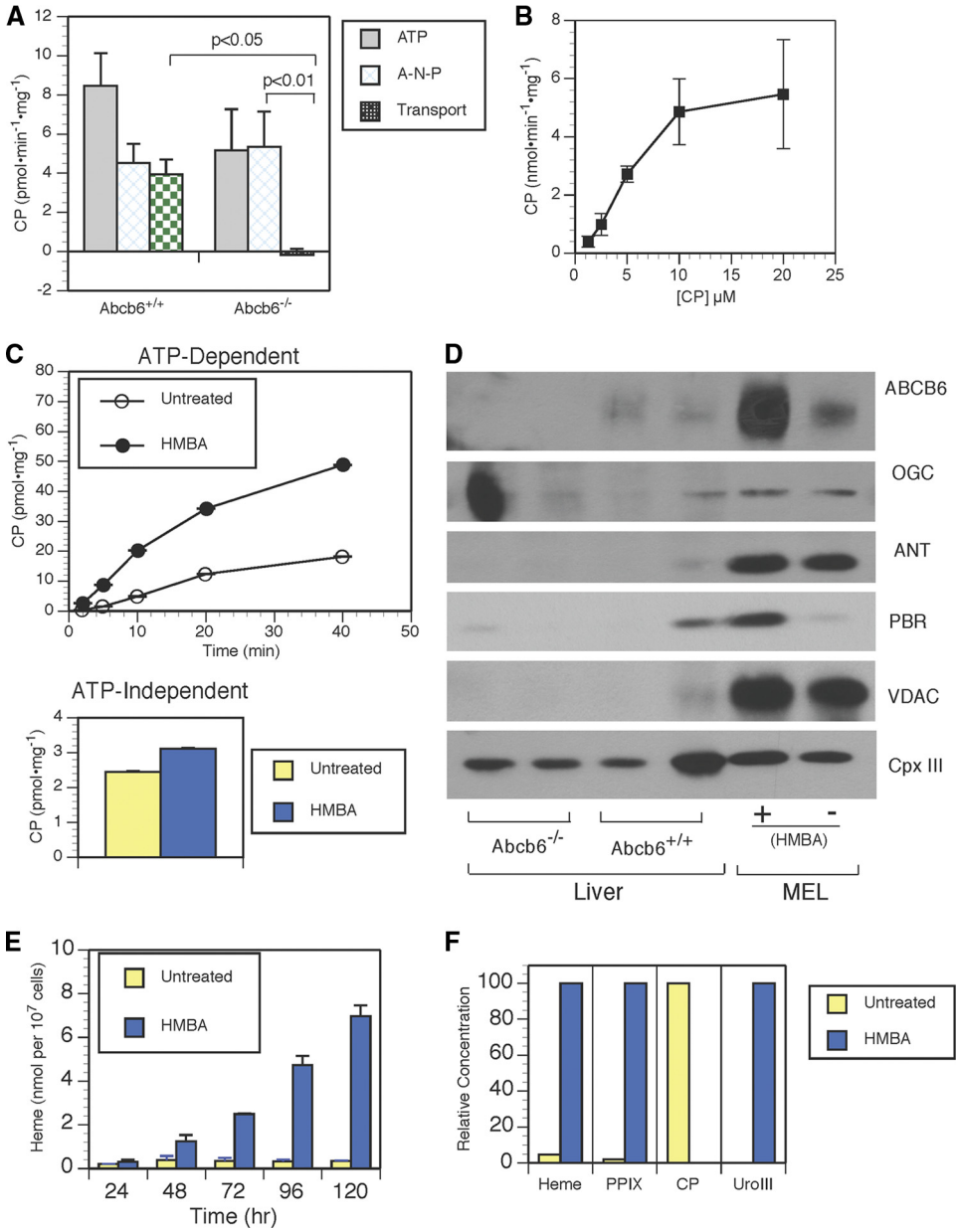

FIGURE 2. **Abcb6 is the sole ATP-dependent mitochondrial transporter of coporphyrin III.** *A,* comparison of CP import in wild-type and *Abcb6*$^{-/-}$ mice, showing ATP-dependent transport (*ATP*), non-ATP-dependent transport (*A-N-P*), and total transport (ATP transport with non-ATP transport subtracted). *B,* import kinetics of CP in mitochondria isolated from mouse liver. *C,* comparison of rate of CP import into untreated and HMBA-treated MEL cells. *D,* immunoblot of mitochondrial lysates shows that non-ATP-dependent carriers are not up-regulated in *Abcb6*$^{-/-}$ mitochondria and that Abcb6 is maximally up-regulated in HMBA-treated MEL cells. *E,* time course of heme concentration in untreated and HMBA-treated MEL cells, as measured by HPLC and normalized by cell number. *F,* HPLC analysis of intracellular porphyrins in untreated and HMBA-treated MEL cells. *VDAC*, voltage-dependent anion channel; *PBR*, peripheral benzodiazepine receptor; *OGC*, 2-oxoglutarate carrier; *ANT*, adenine nucleotide translocator; *Cpx III*, coproporphyrin III.

with the weak affinity of peripheral benzodiazepine receptor for CP compared with hemin or PPIX (Fig. 2*C*). Moreover, immunoblot analysis showed no greater mitochondrial expression of other non-ATP-dependent porphyrin importers, voltage-dependent anion channel, ANT1, or 2-oxoglutarate carrier, in *Abcb6*$^{-/-}$ mice than in wild-type mice (Fig. 2*D*). The increased CP transport we observed in HMBA-treated MEL cells corresponded to a 20-fold increase in heme (measured by HPLC) during the same time course of differentiation (Fig. 2*E* and supplemental Fig. S2). Although small amounts of heme accumulate in the uninduced MEL cells, it is most notable that endogenous coproporphyrinogen III only accumulates in the noninduced cells and not in the MEL cells in which Abcb6 was strongly induced. Together, these data indicate that Abcb6 is required for ATP-dependent mitochondrial import of CP and that in MEL cells, Abcb6 expression levels parallel increased ATP-dependent CP import. Given the parallel increase in heme and Abcb6 function and expression, these findings suggest that Abcb6 is crucial to coordinating porphyrin and iron pathways to synthesize heme.

Non-Mendelian Inheritance and Increased Erythroid PPIX in Abcb6$^{-/-}$ *Mice*—Although the *Abcb6*$^{-/-}$ mice appeared phenotypically normal, multiple independent intercrosses among *Abcb6*$^{+/-}$ mice (153 viable offspring) yielded 10% fewer mice of

TABLE 1
Non-Mendelian inheritance of the *Abcb6* gene

	Abcb6$^{+/+}$	Abcb6$^{+/-}$	Abcb6$^{-/-}$
Expected % (n)[a]	25% (38.25)[b]	50% (76.5)	25% (38.25)
Observed % (n)	35% (53)	42% (64)	23% (36)

[a] Expected inheritance in a population of 153 is given in parentheses.
[b] $p = 0.02$, Pearson's χ^2 test with 2 degrees of freedom.

TABLE 2
Mean (±S.E.) peripheral blood hematological values in Abcb6$^{+/+}$ and Abcb6$^{-/-}$ mice

	Abcb6$^{+/+}$	Abcb6$^{-/-}$	p value
Hematocrit	34.8 ± 1.2%	36.5 ± 0.9%	0.2465
Hemoglobin	12.0 ± 0.5 g/dl	13.0 ± 0.2 g/dl	0.042
Red cell distribution width	14.3 ± 0.3%	14.7 ± 0.2%	0.2842
Mean corpuscular volume	45.7 ± 0.3 fl	44.7 ± 0.2 fl	0.0083
PPIX (mean fluorescence)	1498 ± 112.6	2122 ± 179.7	0.0064
Reticulocytes	9.5 ± 0.9%	10.5 ± 0.7%	0.3704

the *Abcb6*$^{-/-}$ genotype and of the *Abcb6*$^{+/-}$ genotype than expected (Table 1). Because of the role of Abcb6 in mitochondrial porphyrin transport and regulation of intracellular porphyrins, we examined the peripheral blood parameters of *Abcb6*$^{-/-}$ mice (Table 2). Surprisingly, the mean erythrocyte PPIX concentration was 41% greater in *Abcb6*$^{-/-}$ mice than in their wild-type littermates ($p = 0.006$), although the mean corpuscular volume and hemoglobin differed only slightly. All other hematologic parameters measured were comparable in *Abcb6*$^{+/+}$ and *Abcb6*$^{-/-}$ animals.

Compensatory Changes in Gene Expression in Abcb6$^{-/-}$ *Mice*—The increased erythrocyte PPIX and reduced inheritance of the *Abcb6*-null allele suggested that mice survived by compensation. Other knock-out animals with severe defects in heme synthesis have been observed to survive (20–22), although the mechanisms of compensation have not been identified. In particular, the elevated erythrocyte PPIX in *Abcb6*$^{-/-}$ mice suggested that porphyrin biosynthesis may be altered, possibly leading to alteration of iron usage and other interrelated pathways. To determine whether gene expression is altered in the absence of Abcb6, we compared transcript expression in *Abcb6*$^{-/-}$ and wild-type erythroblasts (MACS-purified Ter119-positive cells) by using an Affymetrix microarray (Fig. 3). Pathway analysis (GENEGO, KEGG, and Gseap) indicated the highest ranked pathways were in the porphyrin metabolism and oxidative phosphorylation pathways ($p = 2.18 \times 10^{-12}$ and 2.04×10^{-9}, respectively), consistent with the known role of Abcb6 in activating heme synthesis and with the up-regulation of Abcb6 during erythroid development (10, 17).

To determine the relationship of these genes to heme biosynthesis, we adapted an expression screening approach described by Nilsson *et al.* (11). Analysis of public gene expression datasets available on GEO (23) revealed that during erythroid differentiation *Abcb6* is up-regulated in parallel with many of the eight heme pathway (*alas2, alad, hmbs, uros, urod, cpox, ppox,* and *fech*) genes (Fig. 3*A*). We focused on the 69 mitochondrial and known erythroid-associated genes (of 175) that were up-regulated by a factor of 2 or more in *Abcb6*$^{-/-}$ erythroblasts, plus eight other heme pathway genes (supplemental Table S1), of the total of more than 3500 genes, whose expression was altered by a factor of 2 or more (Fig. 3*B* and supplemental Table S2). Nearly all of the 69 genes were independently verified by ABI gene card analysis (supplemental Fig. S3). Thus, a total of 72 candidate genes were examined within a collection of 314 microarray datasets (supplemental Table S3) representing a wide range of erythropoiesis-relevant conditions. The dataset weight and individual rankings were used to select candidate genes whose expression was highly related to heme gene expression across a range of cell types and experimental conditions as illustrated in Fig. 3*C*. Many of the highest ranking genes in our final list (the top 20 candidates) were potential EKLF targets (24), as supported by putative EKLF-binding sites within 1 kb upstream (supplemental Table S4). Furthermore, heme biosynthetic pathway genes such as *Alas2* and *Hmbs* are known to have EKLF-binding sites, and there is evidence of endogenous binding to EKLF (25, 26). Importantly, *Abcb6* has *bona fide* EKLF-binding sites (supplemental Table 4 and supplemental Fig. S4*A*) and is activated by EKLF (supplemental Fig. S4*B*).

Elevation of EKLF and FECH in Abcb6$^{-/-}$ *Erythroid Cells*—Several transcription factors with known roles in erythropoiesis (EKLF, Nfe2, and MyD116) were expressed more highly in *Abcb6*$^{-/-}$ than in *Abcb6*$^{+/+}$ erythroid cells (supplemental Table S1). However, EKLF was the transcription factor with the highest integrated p value in the expression screen of those that play a role in regulating heme biosynthetic genes (Table 3). Furthermore, EKLF expression was strongly up-regulated, and FECH protein was increased in *Abcb6*$^{-/-}$ mice (Fig. 4*A*), consistent with the observed elevation of FECH mRNA and the fact that FECH is a known EKLF target (27).

Impaired Stress Erythropoiesis in Abcb6$^{-/-}$ *Mice*—The elevated PPIX levels and up-regulation of heme biosynthetic genes in the *Abcb6*$^{-/-}$ mice suggested erythroid cells might not respond to an increased demand in porphyrin synthesis. To determine this, we induced porphyrin synthesis *in vivo*, and mice were injected subcutaneously with phenylhydrazine (Phz, 50 mg/kg) on days 0, 1, and 3 and monitored from day 0 to 8–10. Unexpectedly, *Abcb6*$^{-/-}$ mice showed greater mortality during days 3–7 post-Phz (25/58 or 43% *versus* 11/40 or ~27% in wild-type mice) ($p = 0.043$, two-tailed χ^2 test) (Fig. 4*B*). The *Abcb6*$^{-/-}$ mice that died during days 3–7 had an overall lower mean hematocrit (12.8 *versus* 16%) at day 3 and a greater rate of hematocrit decline than did survivors. Surviving *Abcb6*$^{-/-}$ mice had hematocrits almost identical to those of *Abcb6*$^{+/+}$ mice through day 3, when they reached a nadir of 17.4 ± 1.2% (*Abcb6*$^{+/+}$) and 18.5 ± 0.7% (*Abcb6*$^{-/-}$). However, the time to maximal recovery was significantly delayed in the surviving *Abcb6*$^{-/-}$ mice (day 10 *versus* day 7, $p = 0.004$) (Fig. 4*C*), and the reticulocyte count remained elevated (Fig. 4*D*), indicating that Abcb6 is required for a normal stress response in erythroid cells. The greater red cell distribution width in *Abcb6*$^{-/-}$ mice after day 7 reflected their greater number of reticulocytes, which are larger than erythrocytes (Fig. 4*E*). These findings suggest that *Abcb6*$^{-/-}$ mice remain anemic longer than *Abcb6*$^{+/+}$ mice, consistent with their lower hemoglobin levels during days 5–10 (Fig. 4*F*). Mean corpuscular volume values, which were slightly lower in the *Abcb6*$^{-/-}$ mice before treatment, remained lower during days 3–10, consistent with hemoglobin levels (Fig. 4*G*). These results demonstrate that loss of Abcb6 impairs the normal erythroid response to phenylhydrazine.

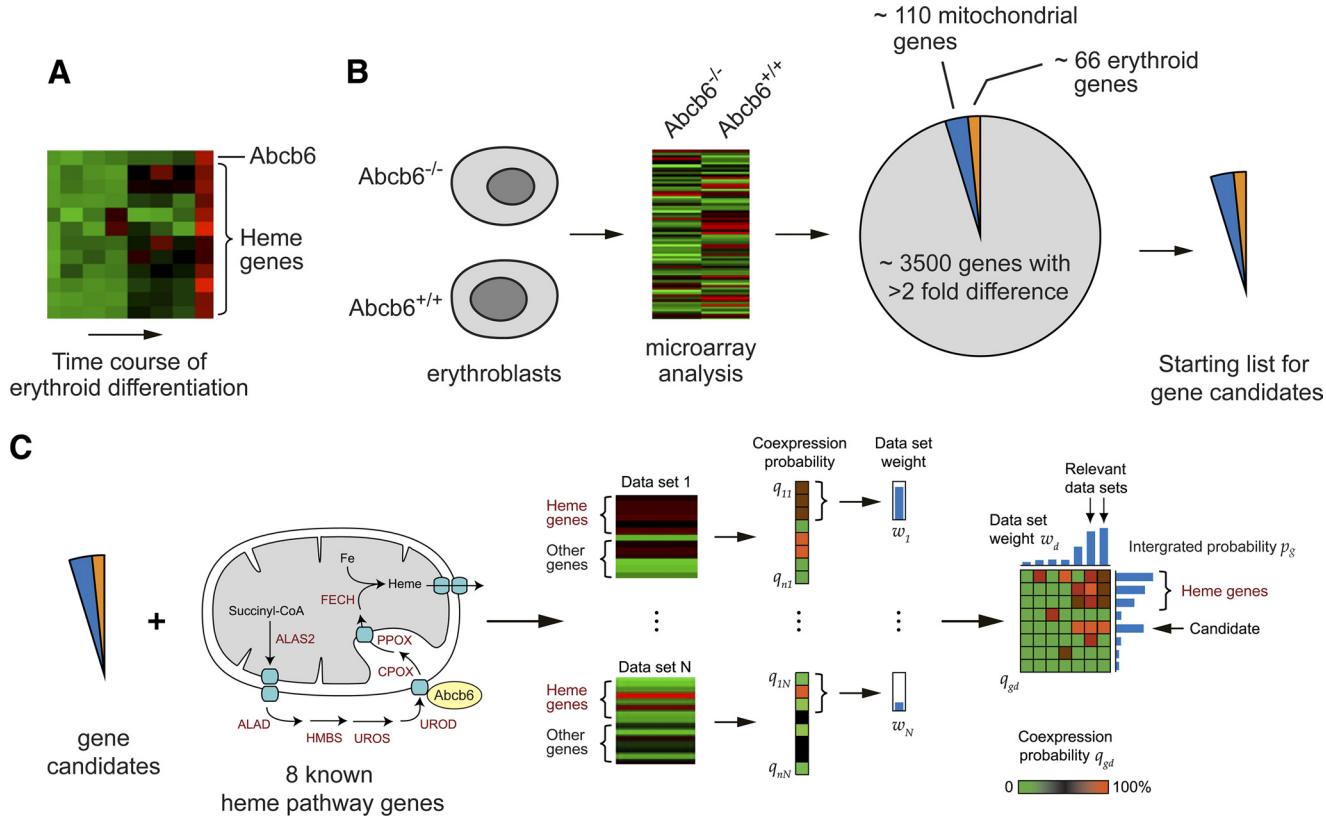

FIGURE 3. **Gene expression screening of *Abcb6*$^{-/-}$ mice.** *A,* during *in vitro* erythroid differentiation, *Abcb6* is up-regulated simultaneously with heme biosynthesis genes. *B,* transcripts were compared in erythroblasts from 1-month-old female wild-type and *Abcb6*$^{-/-}$ mice. Genes whose expression changed by a factor of 2 or more included more than 110 mitochondrial genes and 66 known erythroid-associated genes (candidate genes). *C,* more than 314 arrays were searched to identify genes consistently coexpressed with the candidate genes.

Erythropoietin and Red Blood Cell Turnover—The reticulocytosis observed in *Abcb6*$^{-/-}$ mice might be caused by an overproduction of erythropoietin or by altered differentiation and maturation of erythroid progenitors. *Abcb6*$^{+/+}$ and *Abcb6*$^{-/-}$ mice had similarly elevated serum erythropoietin concentration at day 8, followed by a return to normal levels by day 10 (Fig. 5*A*), ruling out sustained erythropoietin elevation as the primary cause of the prolonged reticulocytosis.

To determine whether reduced cell survival caused the prolonged reticulocytosis and delayed hematocrit recovery, we measured red cell turnover by injecting mice with *N*-hydroxysuccinimide-biotin at day 7 (peak reticulocyte production; see Fig. 4*C*) and monitoring the proportion of *N*-hydroxysuccinimide- and Ter119-positive cells. The mean half-life of Ter119-positive cells did not differ substantially in wild-type and *Abcb6*$^{-/-}$ mice (10.46 *versus* 10.39 days) (Fig. 5*B*). We also found no significant difference between the genotypes in apoptosis of Ter119^{+} cells from spleen and bone marrow during recovery from Phz treatment (Fig. 5*C*).

Because the spleen becomes the primary erythroid organ during Phz-induced stress erythropoiesis in mice (28), we also examined splenic reticulocyte levels during recovery. At day 8, the percentage of reticulocytes in *Abcb6*$^{-/-}$ spleens was more than eight times that in wild-type spleens (Fig. 5*D*). We also examined erythroid colony-forming units (CFU-E), the rapidly divided progenitors that differentiate into orthochromic erythroblasts and then into reticulocytes (29). Untreated wild-type and *Abcb6*$^{-/-}$ mice showed comparable capacity to form CFU-E (Fig. 5*E*), consistent with equal distribution of bone marrow and spleen progenitors expressing the maturation markers CD71 and Ter119 (supplemental Fig. S5). However, splenocytes from Phz-treated *Abcb6*$^{-/-}$ mice showed a significant increase in CFU-E during recovery (Fig. 5*E*), consistent with the observed elevation of reticulocytes and suggesting an intrinsic dysregulation of porphyrin synthesis in *Abcb6*$^{-/-}$ mice is associated with a defect in erythroid maturation.

Elevated PPIX and Deficient Heme Production in Abcb6$^{-/-}$ *Mice*—Because erythroid-cell PPIX was elevated in untreated *Abcb6*$^{-/-}$ mice, we measured PPIX concentration in peripheral and splenic erythroid cells during and after Phz treatment (Fig. 6). The erythrocyte PPIX concentration was approximately twice as high in *Abcb6*$^{-/-}$ mice as in wild-type mice during days 7–10 after Phz treatment (Fig. 6*A*). PPIX concentration was also elevated in *Abcb6*$^{-/-}$ splenic erythroid cells (Fig. 6*B*), particularly in splenic reticulocytes (1.9 times that in wild-type splenic reticulocytes on day 10).

If the *Abcb6*$^{-/-}$ mouse erythrocyte heme-to-PPIX ratio is altered it might suggest a defect in conversion of PPIX to heme. The *Abcb6*$^{-/-}$ heme-to-PPIX ratio was less than 25% that in wild-type mice at days 8 and 10, as was the reticulocyte heme concentration at day 10 (Fig. 6, *C* and *D*). Although FECH is elevated in *Abcb6*$^{-/-}$ mice, it might be nonfunctional. FECH uses Zn^{2+} as a cofactor when iron is insufficient. The ratio of ZnPP to heme provides an *in vivo* measure of the iron available

TABLE 3
The final 72 candidates identified by gene expression screening

Gene	Description	Integrated probability	EKLF target[a]	Unique heme biosynthetic genes[b]	Mitochondrial
CPOX	Coproporphyrinogen oxidase	0.999	X	X	X
FECH	Ferrochelatase	0.999	X	X	X
HMBS	Hydroxymethylbilane synthase	0.999	X	X	X
EKLF	Krüppel-like factor 1 (erythroid)	0.999	X		
UROD	Uroporphyrinogen decarboxylase	0.999	X	X	
PPOX	Protoporphyrinogen oxidase	0.999			X
UROS	Uroporphyrinogen III synthase	0.999		X	
NFE2	Nuclear factor, erythroid-derived 2	0.998	X		
EG623818	Predicted gene, EG623818 HMBS	0.998			
ALAD	Aminolevulinate dehydratase	0.998			
ALAS2	Aminolevulinate, δ-synthase 2	0.997			X
ICAM4	Intercellular adhesion molecule 4	0.996	X		
EIF2AK1	Eukaryotic translation initiation factor 2α kinase 1	0.993			
GLRX5	Glutaredoxin 5 homolog (*Saccharomyces cerevisiae*)	0.992		X	X
EG627557	Predicted gene, EG627557	0.989		X	X
BLVRB	Biliverdin reductase B	0.988	X		
BZRPL1	Benzodiazepine receptor, peripheral-like 1	0.986			
TXNRD2	Thioredoxin reductase 2	0.984		X	X
PCX	Pyruvate carboxylase	0.981	X		X
EPB4.1	Erythrocyte protein band 4.1	0.981			
TFRC	Transferrin receptor	0.977	X		
HSCB	HscB iron-sulfur cluster co-chaperone homolog (*Escherichia coli*)	0.977			X
MTHFD2	Methylenetetrahydrofolate dehydrogenase 2	0.976			X
CD24A	CD24a antigen	0.975	X		
MGST3	Microsomal glutathione *S*-transferase 3	0.971	X		
SLC25A38	Solute carrier family 25, member 38	0.968			X
TSPO	Translocator protein	0.96	X		X
BNIP3L	BCL2/adenovirus E1B interacting protein 3-like	0.96			X
ATPIF1	ATPase inhibitory factor 1	0.957		X	X
ABCG2	ATP-binding cassette, sub-family G (WHITE), member 2	0.951			
HAGH	Hydroxyacyl glutathione hydrolase	0.95		X	X
MCART1	Mitochondrial carrier triple repeat 1	0.945		X	X
HBB-BH1	Hemoglobin Z, β-like embryonic chain	0.94	X		
GLUL	Glutamate-ammonia ligase (glutamine synthetase)	0.92			X
NDUFB9	NADH dehydrogenase (ubiquinone) 1 b 9	0.918			X
MGLL	Monoglyceride lipase	0.916	X		
PRDX2	Peroxiredoxin 2	0.909	X	X	X
EPB4.9	Erythrocyte protein band 4.9	0.908	X		
HK1	Hexokinase 1	0.901		X	X
MYD116	Myeloid differentiation primary response gene 116	0.877	X		
SLC48A1	Solute carrier family 48 (Hrg1)	0.875			
HAX1	HCLS1 associated X-1	0.874			X
BPGM	2,3-Bisphosphoglycerate mutase	0.857			
GMPR	Guanosine monophosphate reductase	0.841	X		
RFESD	Rieske (Fe-S) domain containing	0.826			
ISCA1	Iron-sulfur cluster assembly 1 homolog (*S. cerevisiae*)	0.824		X	X
NT5C3	5′-Nucleotidase, cytosolic III	0.808		X	X
COX7A2	Cytochrome *c* oxidase, subunit VIIa 2	0.754			X
SLC25A37	Solute carrier family 25, member 37	0.75		X	X
FTH1	Ferritin heavy chain 1	0.747			
HBB-Y	Hemoglobin Y, β-like embryonic chain	0.736			
SOD2	Superoxide dismutase 2, mitochondrial	0.733			X
COX5B	Cytochrome *c* oxidase, subunit Vb	0.731			X
ATP5L	ATP synthase mitochondrial F_0 complex	0.709			X
FARS2	Phenylalanine-tRNA synthetase 2 (mitochondrial)	0.653			X
MRS2	Magnesium homeostasis factor homolog (*S. cerevisiae*)	0.648			X
GPX4	Glutathione peroxidase 4	0.629	X		
SLC25A39	Solute carrier family 25, member 39	0.591		X	X
ATP5K	ATP synthase, F_1F_0 complex, subunit e	0.543			X
2010107E04RIK	RIKEN cDNA 2010107E04 gene	0.53			X
COX6A1	Cytochrome *c* oxidase, subunit VI a, polypeptide 1	0.516			X
AIP	Aryl hydrocarbon receptor-interacting protein	0.503			X
LARS2	Leucyl-tRNA synthetase, mitochondrial	0.486			X
BCL2L1	BCL2-like 1	0.443			X
EBF3	Early B-cell factor 3	0.428			
COX6C	Cytochrome *c* oxidase, subunit VIc	0.425			X
UQCRH	Ubiquinol-cytochrome *c* reductase hinge protein	0.419			X
ACTB	Actin, β	0.415			
NDN	Necdin (Ndn), mRNA	0.41			
THSD7B	Thrombospondin, type I, domain containing 7B	0.398	X		
ISCU	IscU iron-sulfur cluster scaffold homolog (*E. coli*)	0.364			X
FIS1	Fission 1 homolog (yeast)	0.272			X

[a] Data are from Drissen *et al.* (24).
[b] Data are from Nilsson *et al.* (11).

for erythropoiesis rather than of general iron stores (30). This ratio increases when mitochondrial iron delivery is impaired and is an early indicator of iron-deficient erythropoiesis (30–32). The ZnPP-to-heme ratio in *Abcb6*$^{-/-}$ animals was more than twice that in wild-type animals post-Phz (Fig. 6*E*), suggesting an inability to meet the demand for mitochondrial iron. We determined if this was a systemic defect in iron absorption by measuring serum iron and transferrin levels. The comparable levels in *Abcb6*$^{-/-}$ and *Abcb6*$^{+/+}$ mice (supplemental Fig. S6) indicate a systemic defect in iron absorption is unlikely. This deficiency is likely to be caused by defective mitochondrial iron regulation.

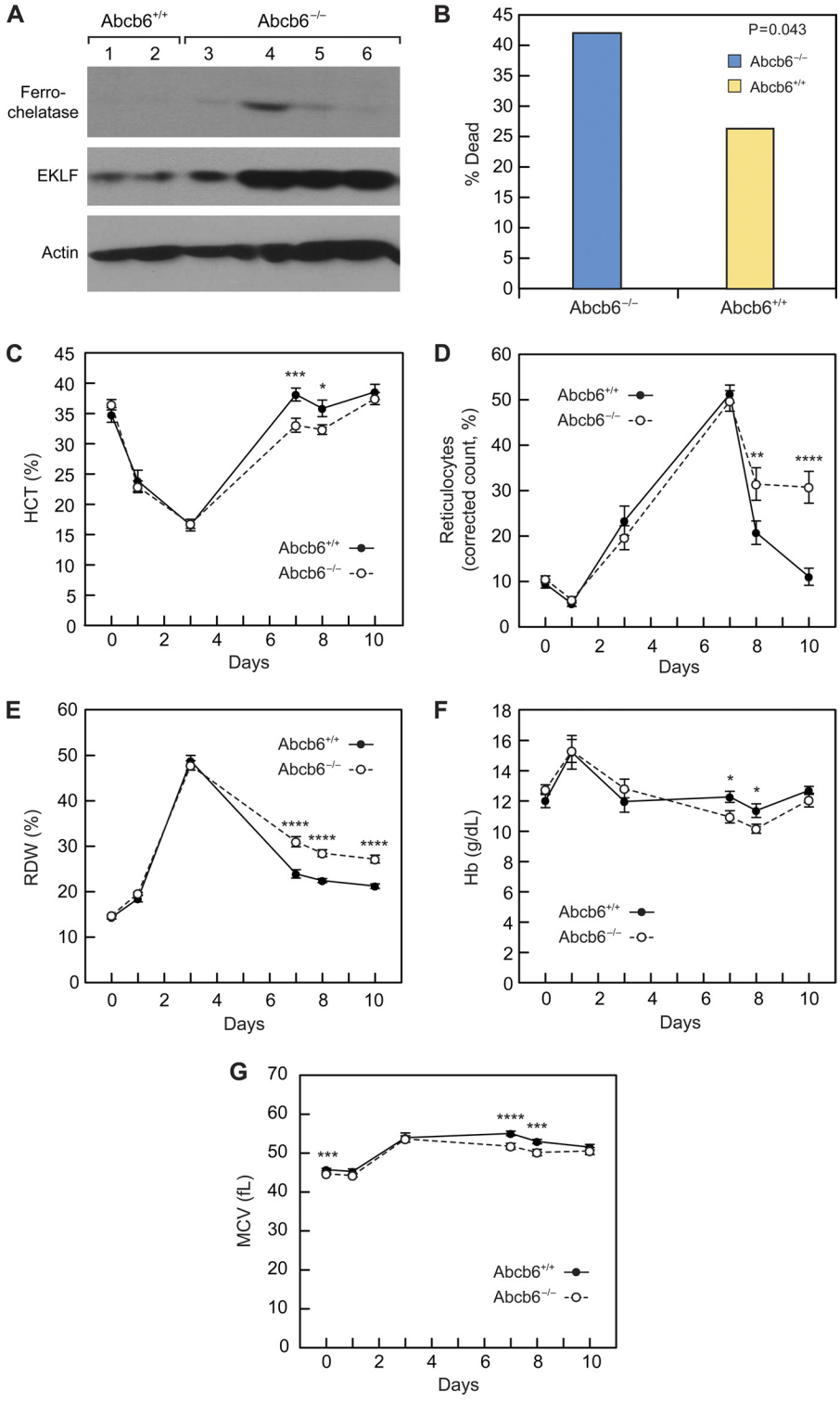

FIGURE 4. **Increased mortality and impaired stress erythropoiesis in *Abcb6*$^{-/-}$ mice.** *A,* EKLF and FECH protein expression is greater in *Abcb6*$^{-/-}$ than *Abcb6*$^{+/+}$ hematopoietic cells. *B,* mortality on days 3–7 of Phz treatment. *C–F,* mean (±S.E.) hematologic parameters of 1-month-old female mice injected with Phz on days 0, 1, and 3 (total dose, 50 mg/kg). *C,* hematocrit (n = 11–30 *Abcb6*$^{+/+}$, 13–46 *Abcb6*$^{-/-}$ mice). *D,* corrected reticulocyte count (n = 9–25 *Abcb6*$^{+/+}$, 12–37 *Abcb6*$^{-/-}$ mice). *E,* red cell distribution width (*RDW*) (n = 10–26 *Abcb6*$^{+/+}$, 13–44 *Abcb6*$^{-/-}$ mice). *F,* hemoglobin (n = *10–26 Abcb6*$^{+/+}$, 13–42 *Abcb6*$^{-/-}$ mice). *G,* mean corpuscular volume (*MCV*) (n = 8–27 *Abcb6*$^{+/+}$, 9–38 *Abcb6*$^{-/-}$ mice). *, p = 0.02–0.03; **, p = 0.01–0.02; ***, p = 0.003–0.009; ****, p = <0.002.

Gene Expression Changes after Phenylhydrazine Treatment—We hypothesized that the up-regulated genes in the *Abcb6*$^{-/-}$ mice might not be regulated appropriately under Phz stress. To test this proposition, we compared gene transcripts in erythroblasts from *Abcb6*$^{+/+}$ and *Abcb6*$^{-/-}$ mice before and 10 days after Phz treatment (Fig. 7 and supplemental Table S1). Many of the genes found to be up-regulated during stress erythropoiesis (by a factor of 1.5 or more) in *Abcb6*$^{+/+}$ erythroblasts were the same genes constitutively up-regulated in the untreated *Abcb6*$^{-/-}$ mice (Table 3). During Phz stress, the *Abcb6*$^{-/-}$

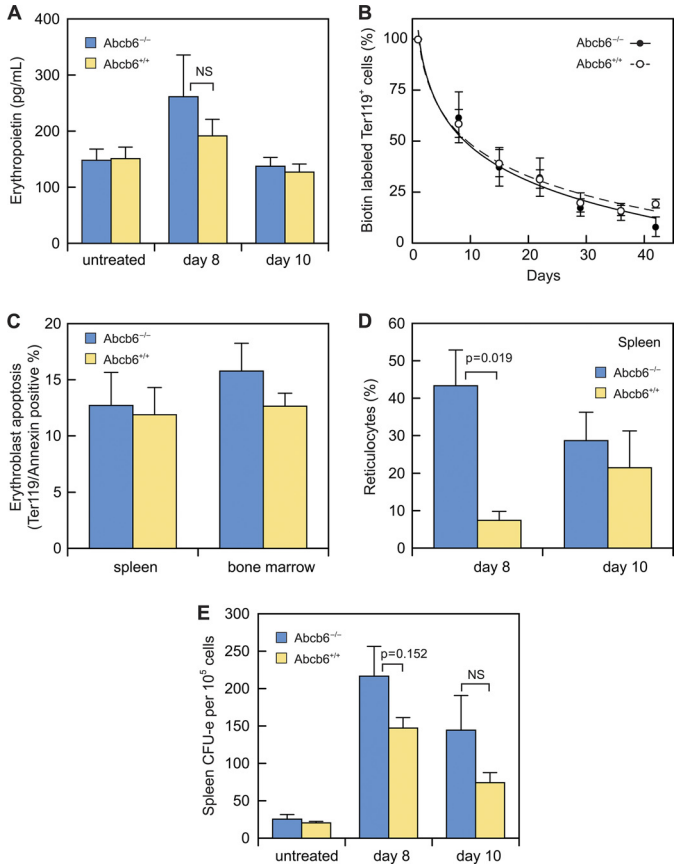

FIGURE 5. **Erythroblast response to stress erythropoiesis is altered in *Abcb6*$^{-/-}$ mice.** *A,* serum erythropoietin assayed by ELISA in *Abcb6*$^{+/+}$ mice that were untreated ($n = 7$), at day 8 of Phz treatment ($n = 5$), or at day 10 of Phz treatment ($n = 5$) and in *Abcb6*$^{-/-}$ mice that were untreated ($n = 7$), at day 8 of Phz treatment ($n = 4$), or at day 10 of Phz treatment ($n = 8$). *B,* duration of erythrocyte survival in 2–4 *Abcb6*$^{+/+}$ and 6–7 *Abcb6*$^{-/-}$ Phz-treated mice. Day 0 of *N*-hydroxysuccinimide-biotin labeling = day 6 or 7 of the Phz regimen. *C,* apoptotic spleen and bone marrow Ter119-positive cells on day 8 of Phz treatment in 9 *Abcb6*$^{+/+}$ and 10 *Abcb6*$^{-/-}$ mice. *D,* percentage of splenic reticulocytes on days 8 and 10 in 3–4 *Abcb6*$^{+/+}$ and 5–6 *Abcb6*$^{-/-}$ mice. *E,* erythroid CFU in spleens of *Abcb6*$^{+/+}$ mice that were untreated ($n = 5$), at day 8 of Phz treatment ($n = 11$), at day 10 of Phz treatment ($n = 9$), and *Abcb6*$^{-/-}$ mice that were untreated ($n = 6$), at day 8 of Phz treatment ($n = 14$), or at day 10 of Phz treatment ($n = 7$) on days 8 and 10. Values are means (±S.E.).

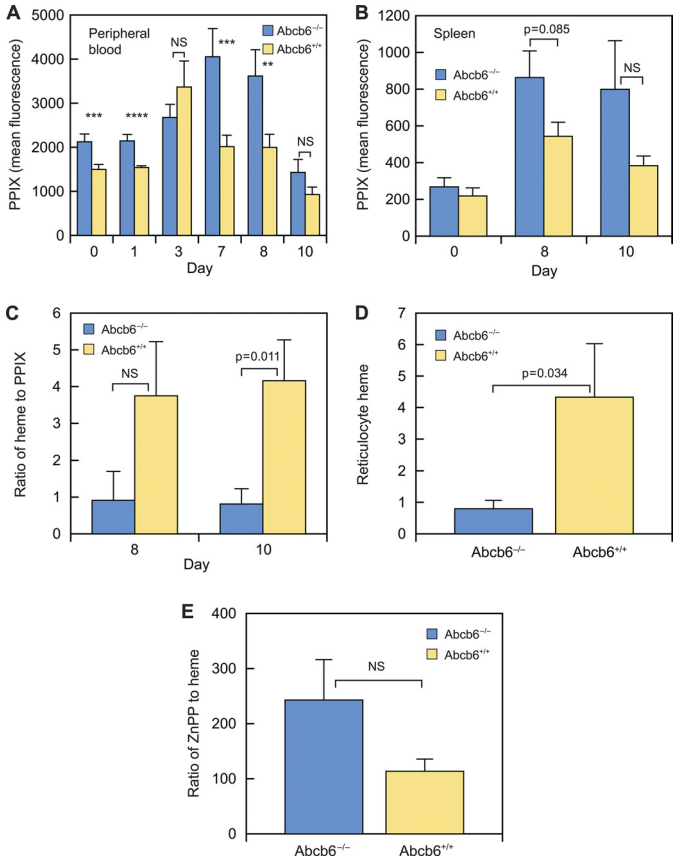

FIGURE 6. **PPIX and ZnPP are elevated in Phz-treated *Abcb6*$^{-/-}$ mice.** *A,* PPIX was assayed in blood samples from 7 to 23 *Abcb6*$^{+/+}$ and 5–26 *Abcb6*$^{-/-}$ mice on the indicated days after treatment. *B,* PPIX in splenic erythroid cells from *Abcb6*$^{+/+}$ mice that were untreated ($n = 8$), at day 8 of Phz treatment ($n = 11$), or at day 10 of Phz treatment ($n = 3$) and from *Abcb6*$^{-/-}$ mice that were untreated ($n = 8$), at day 8 of Phz treatment ($n = 14$), or at day 10 of Phz treatment ($n = 5$). *C,* heme/PPIX ratio in blood from 4 *Abcb6*$^{+/+}$ and 2–6 *Abcb6*$^{-/-}$ mice. *D,* reticulocyte heme on day 10 of Phz treatment in 4 *Abcb6*$^{+/+}$ and 6 *Abcb6*$^{-/-}$ mice. *E,* ZnPP/heme ratio on day 10 in blood from 4 *Abcb6*$^{+/+}$ and 4 *Abcb6*$^{-/-}$ mice. Values are means ±S.E. **, $p = 0.01–0.02$; ***, $p = 0.003–0.009$; ****, $p = 0.002$. *NS*, not significant.

erythroblasts showed either no change or reduced expression of these genes (including *fech, blvrb, cpox, slc48a1, EKLF, nfe2,* and *eif2ak1*), indicating that genes that are important in stress erythropoiesis are constitutively up-regulated in the absence of *Abcb6*.

DISCUSSION

We have presented the first evidence that Abcb6 is the sole mammalian ATP-dependent mitochondrial porphyrin importer and is required for normal porphyrin synthesis during phenylhydrazine stress. Non-ATP-dependent mitochondrial porphyrin transport was not enhanced in the absence of Abcb6, indicating that basal levels of such transport are sufficient for unstressed survival. We demonstrated that in erythroid cells, loss of Abcb6 is compensated for by up-regulation of multiple genes in the porphyrin biosynthetic pathway. Although these changes appear sufficient for survival under normal conditions, the increased mortality, elevated PPIX levels, and decreased production of heme in *Abcb6*$^{-/-}$ mice suggest that Abcb6 is crucial to surviving some stresses.

In view of our previous finding that loss of one *Abcb6* allele in embryonic stem cells was associated with reduced PPIX levels, it was surprising to find elevated PPIX in Abcb6$^{-/-}$erythroid cells. However, loss of Abcb6 is associated with constitutive changes in gene expression that are consistent with conservation of porphyrins. The elevated porphyrins and altered gene expression do not produce overt effects in viable *Abcb6*-null mice under normal conditions. However, the deleterious effects of these adaptive changes become apparent during chemically induced acute stress erythropoiesis, *i.e.* greater mortality and a more sustained anemia associated with reduced erythroid heme concentration despite elevated PPIX. Elevated PPIX can result from iron deficiency or from defective function of FECH (22), the final enzyme in the heme pathway. FECH incorporates iron into the porphyrin ring of PPIX in the presence of an iron-sulfur cluster (ISC) (33). Under normal conditions, serum and tissue iron levels are similar in *Abcb6*$^{+/+}$ and *Abcb6*$^{-/-}$ mice, arguing against a general iron storage defect or malabsorption of dietary iron. Systemic iron usage appears to be unimpaired

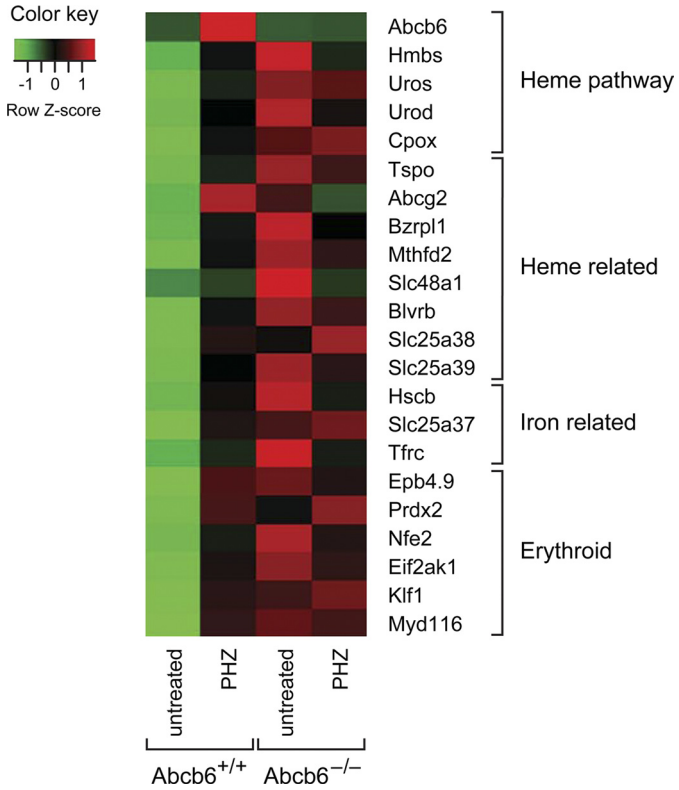

FIGURE 7. ***Abcb6*$^{-/-}$ mouse erythroblasts show impaired up-regulation of heme biosynthetic, ISC, and iron homeostasis genes.** Many genes identified in the expression screening analysis were up-regulated during stress erythropoiesis (day 10 after the start of Phz treatment) in wild-type mice but not in *Abcb6*$^{-/-}$ mice. Each microarray contained RNA from 2 to 4 erythroblast samples.

after stress erythropoiesis, as serum iron and transferrin levels in *Abcb6*$^{-/-}$ and *Abcb6*$^{+/+}$ mice are similar at that time. Defective FECH activity could explain the increased PPIX, but the increase in ZnPP indicates that FECH is functional (23, 34), ruling out defective FECH.

The basal up-regulation of many heme and iron genes in the *Abcb6*$^{-/-}$ mice strongly resembled that in the wild-type mice after phenylhydrazine treatment. However, loss of Abcb6 is associated with up-regulation of many ISC biogenesis genes. In vertebrates, *GIrx5* deficiency provided the first indication that ISC biogenesis and heme biosynthesis are related (35, 36). Of these, *Glrx5*, *Isca1*, *Rfesd*, and *HSCB* showed a strong association (integrated p values >0.82) with the heme biosynthetic genes in our expression screening. We propose that the impaired stress response to phenylhydrazine is partially compensated by up-regulation of *Glrx5* and *Isca1*. However, the inadequate response reflected in a lower survival of *Abcb6*$^{-/-}$ mice suggests compensation is incomplete. Deficiencies in the mitochondrial ISC transporter Abcb7 produces anemia characterized by elevated erythrocyte PPIX and elevated ZnPP-to-heme ratio (37). The lack of change in *Abcb7* gene expression in the *Abcb6*$^{-/-}$ mice suggests this is a potential explanation for poor compensation.

Limitation of a factor required for mitochondrial iron acquisition might also explain the reduced heme in *Abcb6*$^{-/-}$ mice. One potential candidate is Abcb10, a mitochondrial ABC transporter that forms a complex with FECH and the mitochondrial inner membrane transporter Slc25a37 (mitoferrin) (8). Slc25a37 is responsible for importing iron for heme synthesis. Abcb10 interacts with and stabilizes Slc25a37, resulting in increased mitochondrial iron in differentiated MEL cells (38). Targeted deletion of *Abcb10* in mice results in embryonic lethality due to defective erythropoiesis (39). The constitutive level of Abcb10, unlike that of FECH and Slc25a37, is not increased in *Abcb6*$^{-/-}$ erythroid cells. Thus, one possible explanation of impaired heme formation despite adequate PPIX and active FECH is insufficient availability of Abcb10 to form the necessary complexes with FECH and Slc25a37. Under these conditions, decreased mitochondrial iron might account for the reduced heme production.

Other associated gene expression changes suggest that *Abcb6*$^{-/-}$ erythroblasts preserve pre-existing heme within the cell. Our microarray analysis indicated that *Abcb6*$^{-/-}$ erythroblasts express lower levels of heme oxygenase 1 (Hmox 1), which catalyzes heme degradation. This finding is consistent with the observed reduction in heme, which positively regulates Hmox1 (40–42). Slc48a1 (Hrg-1), a heme-binding protein that associates with the endosomes and acts as a heme chaperone (7, 43), was also up-regulated in *Abcb6*$^{-/-}$ erythroblasts, suggesting additional possible mechanisms to conserve heme and maintain iron homeostasis.

Elevated intracellular PPIX is highly cytotoxic to red blood cells and can lead to damage from free radicals. In the disease protoporphyria, excess PPIX causes extensive tissue damage (44). The sustained PPIX levels observed in *Abcb6*$^{-/-}$ red blood cells after phenylhydrazine treatment are a possible explanation for the greater mortality of *Abcb6*$^{-/-}$ mice. The membrane transporter Abcg2 is known to modulate the effects of protoporphyria and may serve to export excess intracellular PPIX, reducing potential cytotoxic damage (1, 44). The increased expression of Abcg2 mRNA in the splenic erythroblasts of *Abcb6*$^{-/-}$ mice may be a survival response to elevated PPIX. As an adaptive change, the increased Abcg2 expression may reduce the concentration of PPIX, under normal conditions. However it's reduction during phenylhydrazine treatment may be insufficient to protect against PPIX-induced cytotoxicity, consistent with the increased mortality observed.

We have shown that the absence of Abcb6 results in loss of ATP-dependent mitochondrial porphyrin import. One implication of these findings is that developmental absence of Abcb6 is survivable, provided rapid porphyrin import is not required. However, given the requirement of functional Abcb6 for an optimal porphyrin metabolism, it is possible that deficiency of Abcb6 (because of mutations or drug inhibitors) contributes to sporadic acute porphyrias.

Acknowledgments—We thank Betsy Williford for figure design; Sharon Naron for excellent editorial assistance; Geoff Neale for Affymetrix analysis; Suraj Mukatira for transcription factor analysis; Mike Straign for assistance with blood samples; Dr. Arthur Nienhuis for critical review of the manuscript; and the staff of the Flow Cytometry and Cell Sorting Shared Resource.

REFERENCES

1. Krishnamurthy, P., and Schuetz, J. D. (2006) Role of ABCG2/BCRP in biology and medicine. *Annu. Rev. Pharmacol. Toxicol.* **46,** 381–410

2. Azuma, M., Kabe, Y., Kuramori, C., Kondo, M., Yamaguchi, Y., and Handa, H. (2008) Adenine nucleotide translocator transports heme precursors into mitochondria. *PLoS One* **3,** e3070
3. Kabe, Y., Ohmori, M., Shinouchi, K., Tsuboi, Y., Hirao, S., Azuma, M., Watanabe, H., Okura, I., and Handa, H. (2006) Porphyrin accumulation in mitochondria is mediated by 2-oxoglutarate carrier. *J. Biol. Chem.* **281,** 31729–31735
4. Vanhee, C., Zapotoczny, G., Masquelier, D., Ghislain, M., and Batoko, H. (2011) The *Arabidopsis* multistress regulator TSPO is a heme-binding membrane protein and a potential scavenger of porphyrins via an autophagy-dependent degradation mechanism. *Plant Cell* **23,** 785–805
5. Wendler, G., Lindemann, P., Lacapère, J. J., and Papadopoulos, V. (2003) Protoporphyrin IX binding and transport by recombinant mouse PBR. *Biochem. Biophys. Res. Commun.* **311,** 847–852
6. Rampon, C., Bouzaffour, M., Ostuni, M. A., Dufourcq, P., Girard, C., Freyssinet, J. M., Lacapere, J. J., Schweizer-Groyer, G., and Vriz, S. (2009) Translocator protein (18 kDa) is involved in primitive erythropoiesis in zebrafish. *FASEB J.* **23,** 4181–4192
7. Rajagopal, A., Rao, A. U., Amigo, J., Tian, M., Upadhyay, S. K., Hall, C., Uhm, S., Mathew, M. K., Fleming, M. D., Paw, B. H., Krause, M., and Hamza, I. (2008) Heme homeostasis is regulated by the conserved and concerted functions of HRG-1 proteins. *Nature* **453,** 1127–1131
8. Chen, W., Dailey, H. A., and Paw, B. H. (2010) Ferrochelatase forms an oligomeric complex with mitoferrin-1 and Abcb10 for erythroid heme biosynthesis. *Blood* **116,** 628–630
9. Krishnamurthy, P., Ross, D. D., Nakanishi, T., Bailey-Dell, K., Zhou, S., Mercer, K. E., Sarkadi, B., Sorrentino, B. P., and Schuetz, J. D. (2004) The stem cell marker Bcrp/ABCG2 enhances hypoxic cell survival through interactions with heme. *J. Biol. Chem.* **279,** 24218–24225
10. Lynch, J., Fukuda, Y., Krishnamurthy, P., Du, G., and Schuetz, J. D. (2009) Cell survival under stress is enhanced by a mitochondrial ATP-binding cassette transporter that regulates hemoproteins. *Cancer Res.* **69,** 5560–5567
11. Nilsson, R., Schultz, I. J., Pierce, E. L., Soltis, K. A., Naranuntarat, A., Ward, D. M., Baughman, J. M., Paradkar, P. N., Kingsley, P. D., Culotta, V. C., Kaplan, J., Palis, J., Paw, B. H., and Mootha, V. K. (2009) Discovery of genes essential for heme biosynthesis through large scale gene expression analysis. *Cell Metab.* **10,** 119–130
12. Feng, W. C., Southwood, C. M., and Bieker, J. J. (1994) Analyses of β-thalassemia mutant DNA interactions with erythroid Krüppel-like factor (EKLF), an erythroid cell-specific transcription factor. *J. Biol. Chem.* **269,** 1493–1500
13. Pilon, A. M., Ajay, S. S., Kumar, S. A., Steiner, L. A., Cherukuri, P. F., Wincovitch, S., Anderson, S. M. NISC Comparative Sequencing Center, Mullikin, J. C., Gallagher, P. G., Hardision, R. C., Margulies, E. H., and Bodine, D. M. (2012) Genome-wide ChIP-Seq reveals a dramatic shift in the binding of the transcription factor erythroid Kruppel-like factor during erythroid differentiation. *Blood* **118,** e139–e148
14. Bieker, J. J., and Southwood, C. M. (1995) The erythroid Krüppel-like factor transactivation domain is a critical component for cell-specific inducibility of a β-globin promoter. *Mol. Cell. Biol.* **15,** 852–860
15. Thomas-Chollier, M., Sand, O., Turatsinze, J. V., Janky, R., Defrance, M., Vervisch, E., Brohée, S., and van Helden, J. (2008) RSAT. Regulatory sequence analysis tools. *Nucleic Acids Res.* **36,** W119–127
16. Emadi-Konjin, H. P., Zhang, H., Anandan, V., Sun, D., Schuetz, J., and Furuya, K. N. (2002) Isolation of a genomic clone containing the promoter region of the human ATP-binding cassette (ABC) transporter, ABCB6. *Biochim. Biophys. Acta* **1574,** 117–130
17. Krishnamurthy, P. C., Du, G., Fukuda, Y., Sun, D., Sampath, J., Mercer, K. E., Wang, J., Sosa-Pineda, B., Murti, K. G., and Schuetz, J. D. (2006) Identification of a mammalian mitochondrial porphyrin transporter. *Nature* **443,** 586–589
18. Koller, M. E., and Romslo, I. (1980) Uptake of protoporphyrin IX by isolated rat liver mitochondria. *Biochem. J.* **188,** 329–335
19. Rebeiz, N., Arkins, S., Kelley, K. W., and Rebeiz, C. A. (1996) Enhancement of coproporphyrinogen III transport into isolated transformed leukocyte mitochondria by ATP. *Arch. Biochem. Biophys.* **333,** 475–481
20. Cooperman, S. S., Meyron-Holtz, E. G., Olivierre-Wilson, H., Ghosh, M. C., McConnell, J. P., and Rouault, T. A. (2005) Microcytic anemia, erythropoietic protoporphyria, and neurodegeneration in mice with targeted deletion of iron-regulatory protein 2. *Blood* **106,** 1084–1091
21. Crooks, D. R., Ghosh, M. C., Haller, R. G., Tong, W. H., and Rouault, T. A. (2010) Post-translational stability of the heme biosynthetic enzyme ferrochelatase is dependent on iron availability and intact iron-sulfur cluster assembly machinery. *Blood* **115,** 860–869
22. Magness, S. T., Maeda, N., Brenner, D. A. (2002) An exon 10 deletion in the mouse ferrochelatase gene has a dominant-negative effect and causes mild protoporphyria. *Blood* **100,** 1470–1477
23. Li, F. M., Lim, C. K., and Peters, T. J. (1987) An HPLC assay for rat liver ferrochelatase activity. *Biomed. Chromatogr.* **2,** 164–168
24. Drissen, R., von Lindern, M., Kolbus, A., Driegen, S., Steinlein, P., Beug, H., Grosveld, F., and Philipsen, S. (2005) The erythroid phenotype of EKLF-null mice. defects in hemoglobin metabolism and membrane stability. *Mol. Cell. Biol.* **25,** 5205–5214
25. Frampton, J., Walker, M., Plumb, M., and Harrison, P. R. (1990) Synergy between the NF-E1 erythroid-specific transcription factor and the CACCC factor in the erythroid-specific promoter of the human porphobilinogen deaminase gene. *Mol. Cell. Biol.* **10,** 3838–3842
26. Kramer, M. F., Gunaratne, P., and Ferreira, G. C. (2000) Transcriptional regulation of the murine erythroid-specific 5-aminolevulinate synthase gene. *Gene* **247,** 153–166
27. Tugores, A., Magness, S. T., and Brenner, D. A. (1994) A single promoter directs both housekeeping and erythroid preferential expression of the human ferrochelatase gene. *J. Biol. Chem.* **269,** 30789–30797
28. Socolovsky, M., Nam, H., Fleming, M. D., Haase, V. H., Brugnara, C., and Lodish, H. F. (2001) Ineffective erythropoiesis in Stat5a(−/−)5b(−/−) mice due to decreased survival of early erythroblasts. *Blood* **98,** 3261–3273
29. Zhang, J., Socolovsky, M., Gross, A. W., and Lodish, H. F. (2003) Role of Ras signaling in erythroid differentiation of mouse fetal liver cells. Functional analysis by a flow cytometry-based novel culture system. *Blood* **102,** 3938–3946
30. Winzerling, J. J., and Kling, P. J. (2001) Iron-deficient erythropoiesis in premature infants measured by blood zinc protoporphyrin/heme. *J. Pediatr.* **139,** 134–136
31. Rettmer, R. L., Carlson, T. H., Origenes, M. L., Jack, R. M., and Labb, R. F. (1999) Zinc protoporphyrin/heme ratio for diagnosis of preanemic iron deficiency. *Pediatrics* **104,** e37
32. Labbé, R. F., Vreman, H. J., and Stevenson, D. K. (1999) Zinc protoporphyrin. A metabolite with a mission. *Clin. Chem.* **45,** 2060–2072
33. Medlock, A. E., and Dailey, H. A. (2000) Examination of the activity of carboxyl-terminal chimeric constructs of human and yeast ferrochelatases. *Biochemistry* **39,** 7461–7467
34. Goerz, G., Bunselmeyer, S., Bolsen, K., and Schürer, N. Y. (1996) Ferrochelatase activities in patients with erythropoietic protoporphyria and their families. *Br. J. Dermatol.* **134,** 880–885
35. Camaschella, C., Campanella, A., De Falco, L., Boschetto, L., Merlini, R., Silvestri, L., Levi, S., and Iolascon, A. (2008) The human counterpart of zebrafish shiraz shows sideroblastic-like microcytic anemia and iron overload. *Blood* **110,** 1353–1358
36. Wingert, R. A., Galloway, J. L., Barut, B., Foott, H., Fraenkel, P., Axe, J. L., Weber, G. J., Dooley, K., Davidson, A. J., Schmid, B., Schmidt, B., Paw, B. H., Shaw, G. C., Kingsley, P., Palis, J., Schubert, H., Chen, O., Kaplan, J., Zon, L. I., and Tübingen 2000 Screen Consortium (2005) Deficiency of glutaredoxin 5 reveals Fe-S clusters are required for vertebrate heme synthesis. *Nature* **436,** 1035–1039
37. Pondarré, C., Antiochos, B. B., Campagna, D. R., Clarke, S. L., Greer, E. L., Deck, K. M., McDonald, A., Han, A. P., Medlock, A., Kutok, J. L., Anderson, S. A., Eisenstein, R. S., and Fleming, M. D. (2006) The mitochondrial ATP-binding cassette transporter Abcb7 is essential in mice and participates in cytosolic iron-sulfur cluster biogenesis. *Hum. Mol. Genet.* **15,** 953–964
38. Chen, W., Paradkar, P. N., Li, L., Pierce, E. L., Langer, N. B., Takahashi-Makise, N., Hyde, B. B., Shirihai, O. S., Ward, D. M., Kaplan, J., and Paw, B. H. (2009) Abcb10 physically interacts with mitoferrin-1 (Slc25a37) to enhance its stability and function in the erythroid mitochondria. *Proc. Natl. Acad. Sci. U.S.A.* **106,** 16263–16268
39. Hyde, B. B., Liesa, M., Elorza, A. A., Qiu, W., Haigh, S. E., Richey, L.,

Mikkola, H. K., Schlaeger, T. M., and Shirihai, O. S. (2012) Mitochondrial transporter ABC-me (ABCB10), a downstream target of GATA-1, is essential for erythropoiesis *in vivo*. *Cell Death Diff.* **19,** 1–10

40. Chen, G. G., Liu, Z. M., Vlantis, A. C., Tse, G. M., Leung, B. C., and van Hasselt, C. A. (2004) Heme oxygenase-1 protects against apoptosis induced by tumor necrosis factor-α and cycloheximide in papillary thyroid carcinoma cells. *J. Cell. Biochem.* **92,** 1246–1256
41. Liu, Z. M., Chen, G. G., Ng, E. K., Leung, W. K., Sung, J. J., and Chung, S. C. (2004) Up-regulation of heme oxygenase-1 and p21 confers resistance to apoptosis in human gastric cancer cells. *Oncogene* **23,** 503–513
42. Lavrovsky, Y., Schwartzman, M. L., Levere, R. D., Kappas, A., and Abraham, N. G. (1994) Identification of binding sites for transcription factors NF-κB and AP-2 in the promoter region of the human heme oxygenase 1 gene. *Proc. Natl. Acad. Sci. U.S.A.* **91,** 5987–5991
43. O'Callaghan, K. M., Ayllon, V., O'Keeffe, J., Wang, Y., Cox, O. T., Loughran, G., Forgac, M., and O'Connor, R. (2010) Heme-binding protein HRG-1 is induced by insulin-like growth factor I and associates with the vacuolar H^+-ATPase to control endosomal pH and receptor trafficking. *J. Biol. Chem.* **285,** 381–391
44. Jonker, J. W., Buitelaar, M., Wagenaar, E., Van Der Valk, M. A., Scheffer, G. L., Scheper, R. J., Plosch, T., Kuipers, F., Elferink, R. P., Rosing, H., Beijnen, J. H., and Schinkel, A. H. (2002) The breast cancer resistance protein protects against a major chlorophyll-derived dietary phototoxin and protoporphyria. *Proc. Natl. Acad. Sci. U.S.A.* **99,** 15649–15654